JACS
JOURNAL OF THE AMERICAN CHEMICAL SOCIETY
Communication
pubs.acs.org/JACS

Luminescent Ce(III) Complexes as Stoichiometric and Catalytic Photoreductants for Halogen Atom Abstraction Reactions

Haolin Yin, Patrick J. Carroll, Jessica M. Anna,* and Eric J. Schelter*

P. Roy and Diana T. Vagelos Laboratories, Department of Chemistry, University of Pennsylvania, 231 South 34 Street, Philadelphia, Pennsylvania 19104, United States

Supporting Information

ABSTRACT: Luminescent Ce(III) complexes, $Ce[N(SiMe_3)_2]_3$ (**1**) and $[(Me_3Si)_2NC(RN)_2]Ce[N(SiMe_3)_2]_2$ (R = ^{i}Pr, **1-^{i}Pr**; R = Cy, **1-Cy**), with C_{3v} and C_{2v} solution symmetries display absorptive 4f → 5d electronic transitions in the visible region. Emission bands are observed at 553, 518, and 523 nm for **1**, **1-^{i}Pr**, and **1-Cy** with lifetimes of 24, 67, and 61 ns, respectively. Time-dependent density functional theory (TD-DFT) studies on **1** and **1-^{i}Pr** revealed the $^2A_1$ excited states corresponded to singly occupied $5d_{z^2}$ orbitals. The strongly reducing metalloradical character of **1**, **1-^{i}Pr**, and **1-Cy** in their $^2A_1$ excited states afforded photochemical halogen atom abstraction reactions from sp^3 and sp^2 C−X (X = Cl, Br, I) bonds for the first time with a lanthanide cation. The dehalogenation reactions could be turned over with catalytic amounts of photosensitizers by coupling salt metathesis and reduction to the photopromoted atom abstraction reactions.

In photoredox chemistry the energy of visible light, especially of high energy blue light (440 nm, 2.8 eV), is absorbed by photosensitizers and converted into redox power for reactivity. Current molecular photosensitizers including $Ru^{II}(bpy)_3^{2+}$ (bpy = 2,2′-bipyridine),[1] *fac*-$Ir^{IV}(ppy)_3^{+}$ (ppy = 2,2′-phenylpyridine),[2] tungsten(0) isocyanides,[3] Cu(I) complexes,[4] and organic dyes,[5] accomplish photoredox reactions exclusively through outer sphere electron transfer processes. Photoreductants activate substrates under mild conditions and have drawn interest in catalysis.[6] For example, in catalytic oxidative quenching cycles,[6d] electrons are transferred from excited-state photosensitizers to acceptors to effect chemical changes. Antibonding orbitals of C−X (X = Cl, Br, I) bonds are one such target, leading to reductive C−X bond cleavage. In such cases, the scope of accessible substrates containing C−X bonds depends solely on the excited state reduction potential of the photosensitizer.[7]

In contrast to outer sphere processes, we hypothesized that favorable M−X bond formation enthalpies could be coupled with metal redox power in an inner sphere electron transfer process, providing additional driving force for the activation of substrates. An inner sphere photosensitizer would require the association of C−X bonds to a metal cation in its excited state. As such, highly electrophilic f-block cations are excellent candidates for such reactivity. Herein, we report the use of luminescent Ce(III) complexes as inner sphere photoreductants for C−X bond activation. Cerium(III) is a redox active cation.[8] With its single 4f electron, Ce(III) complexes have simple, well-defined electronic structures featuring $^2F_{5/2}$ ground states. In fact, reported luminescence of Ce^{3+} cations originates from 5d → 4f transitions,[9] distinct from most other Ln^{3+} cations where 4f → 4f transitions underlie optical properties. The interconfigurational transition shows greater emission intensity but shorter lifetimes compared to other lanthanide cations; the 5d → 4f transition is allowed by both parity and spin selection rules.[10]

We noted that the common Ce(III) protonolysis reagent, $Ce[N(SiMe_3)_2]_3$ (**1**), emitted yellow light weakly under UV irradiation (365 nm). However, treatment of **1** with excess carbodiimides, R−N═C═N−R (R = ^{i}Pr, Cy), afforded isolation of their monoinsertion products, **1-^{i}Pr** and **1-Cy** (Scheme 1), which were found to be bright green emitters. X-ray

Scheme 1. Synthesis of 1-^{i}Pr and 1-Cy from 1

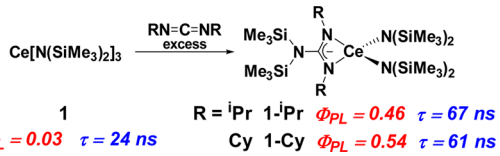

studies confirmed the yellow compounds **1-^{i}Pr** and **1-Cy** as the monoguanidinate insertion products (Figures S3−S4). No further insertion was observed for **1-^{i}Pr** or **1-Cy** with excess carbodiimide to 80 °C.

Electronic absorption spectra of **1-^{i}Pr**, **1-Cy** resembled the spectrum of **1**, displaying two bands with $\varepsilon \approx 300-400\ M^{-1}\ cm^{-1}$ in the visible range attributed to 4f → 5d transitions (Figure 1). The emission energies of **1-^{i}Pr** and **1-Cy** were blue-shifted by ca. 30 nm compared to **1**, resulting in green luminescence. The guanidinate complexes **1-^{i}Pr** and **1-Cy** exhibited relatively high photoluminescence quantum yields Φ_{PL} = 0.46 and 0.54 for **1-^{i}Pr** and **1-Cy**, respectively, compared to **1**: Φ_{PL} = 0.03. Consistent with the observation of a low quantum yield was the short measured lifetime for **1** (24 ns) compared to **1-^{i}Pr** (67 ns) and **1-Cy** (61 ns). No variance of the lifetime was observed across the emission profiles for all complexes, suggesting the emissions originated from a single excited electronic state.[10c] All emission spectra were deconvoluted into pairs of overlapping Gaussian bands (Figures S48−S50), consistent with the transitions from their emissive states to the ^2F ground manifold. The ^2F ground manifold is split by spin−orbital coupling into the $J = 5/2$ ground

Received: May 25, 2015
Published: July 7, 2015

DOI: 10.1021/jacs.5b05411
J. Am. Chem. Soc. 2015, 137, 9234−9237

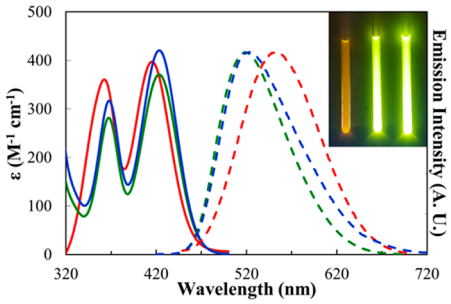

Figure 1. UV−vis electronic absorption spectra (solid lines) and normalized emission spectra (dashed lines) of **1** (red), **1**-^{i}**Pr** (green), **1**-**Cy** (blue) recorded in toluene. Pictures of C_6H_6 solution containing **1** (left), **1**-^{i}**Pr** (middle), and **1**-**Cy** (right) in Pyrex NMR tubes (1.0 mM) under UV irradiation (365 nm) (inset).

state and $J = 7/2$ excited states.[9b] Excitation spectra collected at the emission maxima for **1**, **1**-^{i}**Pr**, **1**-**Cy** showed intense, overlapping bands with their lowest energy 4f → 5d absorption bands at ca. 420 nm (Figures S45−S47), supporting the associated excited state as the long-lived emissive state.

In an effort to identify the frontier orbitals involved in the electronic transitions of **1**, **1**-^{i}**Pr**, and **1**-**Cy**, time-dependent density functional theory (TD-DFT) calculations were performed for complexes **1** and **1**-^{i}**Pr**. The predicted vertical excitations and intensities were in reasonably good agreement with the experimental data, indicating two metal based 4f → 5d transitions (Figure 2). Natural transition orbitals (NTOs)[11] analyses revealed the lowest energy transitions at ca. 420 nm for **1** and **1**-^{i}**Pr** were both from ground states of primarily 4f character to $5d_{z^2}$ orbital-based excited states: $^{2}A_1$ in both the C_{3v} and C_{2v} point groups. The results are readily rationalized as the $5d_{z^2}$ orbitals are essentially nonbonding in both cases and therefore of the lowest energy within the 5d-manifold.[12] The acceptor orbitals of the transition at 341 nm were found to be a degenerate set of $5d_{xz}$ and $5d_{yz}$ orbitals for **1**; such degeneracy is lost for the lower symmetry complex, **1**-^{i}**Pr**. The $^{2}A_1$ states were therefore assigned as the long-lived excited states for all three complexes. Additionally, a ligand-to-metal charge transfer (LMCT) absorption tail located below 320 nm for **1**-^{i}**Pr** was attributed by the TD-DFT result to a guanidinate nonbonding π_n-orbital to 4f-orbital CT transition (Figure S78).

To evaluate the reduction potential of the Ce(III) complexes upon photoexcitation, the excited state potentials ($E^*_{1/2}$) for the $^{2}A_1$ states were approximated using the ground state potentials ($E_{1/2}$) and emission band energies following the Rehn-Weller formalism:[13]

$$E^*_{1/2} = E_{1/2} - E_{0,0}$$

Cyclic voltammetry experiments on **1**-^{i}**Pr** and **1**-**Cy** in CH_2Cl_2 with 0.1 M $[^{n}Pr_4N][BAr^{F}_4]$ as the supporting electrolyte revealed quasi-reversible $Ce^{IV/III}$ couples with $E_{1/2} = +0.03$ V and +0.13 V versus $Cp_2Fe^{+/0}$, respectively (Figures S54−S55). The electrochemical data of **1** in THF ($E_{1/2} = +0.35$ V)[14] were applied for its estimate of the excited state reduction potential because no feature was observed for **1** in CH_2Cl_2. The $E_{1/2}$* values were estimated to be −1.89, −2.36, and −2.24 V versus $Cp_2Fe^{+/0}$ for **1**, **1**-^{i}**Pr**, and **1**-**Cy**, respectively (Table 1), providing opportunities for accessing photoreduction chemistry with Ce(III) complexes.

Based on the spectroscopic and electrochemical data, we hypothesized that combining the reducing power of the $^{2}A_1$ excited state and Ce(IV)−X bond enthalpy would allow us to activate challenging C−X bonds photochemically through an inner sphere atom abstraction pathway. We choose $PhCH_2Cl$ as a first target for activation since the cathodic reduction wave of $PhCH_2Cl$ was reported at $E_{pc} = -2.66$ V versus $Cp_2Fe^{+/0}$ in DMF,[15] lower than the −1.89 V estimated reduction potential for

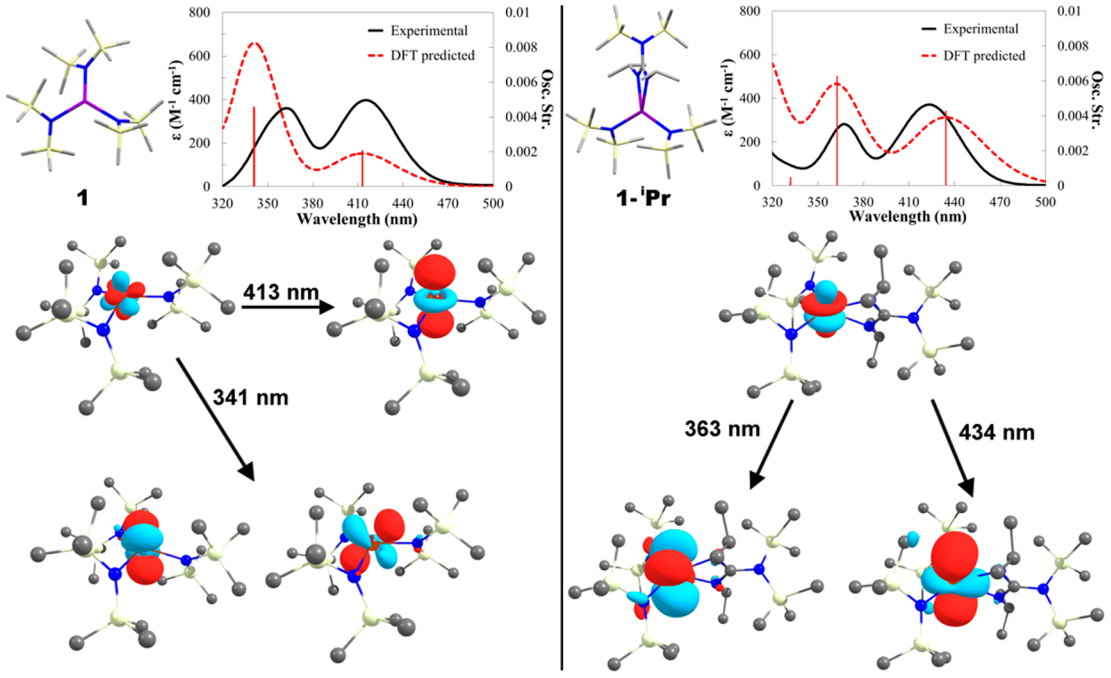

Figure 2. Experimental (black solid lines) and TD-DFT predicted (red dashed lines) absorption spectra of **1** (left) and **1**-^{i}**Pr** (right). The predicted spectra were rendered as Gaussian line shapes having a fwhm of 3000 cm^{-1}. Oscillator strengths for the electronic transitions are shown as red vertical lines. Stick representations of the crystal structures of **1** and **1**-^{i}**Pr** are shown to the left of the spectra. Natural transition orbitals (NTOs) are shown for the donor/acceptor orbitals of each transition.

DOI: 10.1021/jacs.5b05411
J. Am. Chem. Soc. 2015, 137, 9234−9237

Table 1. Estimation of Reduction Potential for Ce(III) $^2A_1$ Excited States

	$E_{1/2}{}^a$/eV	$E_{0,0}$/eV	$E_{1/2}{}^*$/eV
1	+0.35[b]	+2.24	−1.89
1-^{i}Pr	+0.03	+2.39	−2.36
1-Cy	+0.13	+2.37	−2.24

[a]Cyclic voltammetry in 0.1 M [^{n}Pr$_4$N][BAr$^F{}_4$]/CH_2Cl_2. [b]In THF.

1*. Thus, an outer sphere electron transfer process would not be expected to occur between **1*** and $PhCH_2Cl$ on thermodynamic grounds. Combinations of **1** and $PhCH_2Cl$ showed no reaction in the absence of light. Irradiation of a C_6D_6 solution containing **1** with an excess of $PhCH_2Cl$ in a photoreactor equipped with 420 nm narrow band lamps led to a color change of the solution from yellow to dark red/purple within 5 min. The reaction also proceeded with commercially available compact fluorescent lamps (CFLs) as light sources. An ^{1}H NMR experiment showed the formation of $Ce^{IV}Cl[N(SiMe_3)_2]_3$ (**2**), concomitant with the generation of $PhCH_2CH_2Ph$ (Scheme 2) through radical homocoupling.

Similarly, photoreactions of **1-^{i}Pr** (or **1-Cy**) with excess $PhCH_2Cl$ led to color changes from yellow to black (Scheme 2) and the production of $PhCH_2CH_2Ph$ was confirmed by ^{1}H NMR spectroscopy. Also noted in the solution ^{1}H NMR spectra were sets of resonances for the Ce(IV)−Cl products, **2-^{i}Pr** (or **2-Cy**). To confirm the assessments of the oxidation products, **2-^{i}Pr** and **2-Cy** were independently prepared from reactions of Ph_3C−Cl with **1-^{i}Pr** and **1-Cy**. X-ray crystallography studies confirmed their identities as the Ce(IV)−Cl products (Figures S5−S6). The black complexes **2-^{i}Pr** and **2-Cy** are the first examples of κ^2-guanidinate moieties coordinated to Ce(IV) cations; related cerium(III/IV) amidates and formamidinates have been reported.[16] The black appearances of **2-^{i}Pr** and **2-Cy** were evident in their UV−vis spectra, where both compounds were found to absorb evenly in the visible range, 400−800 nm (3.1−1.5 eV, Figure S42). TD-DFT calculations performed on **2-^{i}Pr** afforded assignment of bands in the visible region as LMCT (Figure S89). The computed HOMO → LUMO excitation at 725 nm (1.71 eV) corresponded to a guanidinate nonbonding π orbital (π_n) to a 4f-orbital.

In all cases, the Ce(IV)−Cl products, **2**, **2-^{i}Pr**, and **2-Cy**, were stronger absorbers than their Ce(III) congeners. As such, the Ce(IV) products in the reaction mixture inhibited the absorption of light by Ce(III) species and resulted in incomplete reactions. To avoid accumulation of Ce(IV) species, we found $NaN(SiMe_3)_2$ could effectively reduce the Ce(IV)−Cl products to Ce(III) species with precipitation of NaCl and formation of an aminyl radical: $\cdot N(SiMe_3)_2$. However, under catalytic conditions with stoichiometric $NaN(SiMe_3)_2$, only a low yield (22% in Et_2O) of $PhCH_2CH_2Ph$ was achieved, due to side reactions of the aminyl radical with the starting material, $PhCH_2Cl$. Byproducts, including $PhCH_2N(SiMe_3)_2$ and $PhCH_2CHClPh$, were identified by ^{1}H NMR spectroscopy and GC-MS (see Figures S22, S30−S34). To address these problems, Zn or Ce metal powders were introduced to the reaction mixtures as additives to quench the aminyl radical and afforded bibenzyl products in reasonable yields; control experiments showed slow background reactions of the metal powders with $PhCH_2Cl$ (Scheme 3 and Table S1). Further controls demonstrated the metal powders reacted slowly with **2**; direct reaction of $NaN(SiMe_3)_2$ with **2** proceeded instantaneously.

Scheme 3. $PhCH_2Cl$ Coupling Reactions with Ce-Metal as External Reductant

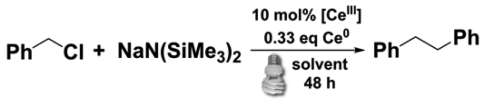

Entry	[Ce^{III}]	Solvent	Yield[a]/%
1	**1**	Et_2O	68
2	**1-^{i}Pr**	Et_2O	17
3	**1-Cy**	Et_2O	10
4	-	Et_2O	5
5	**1**	C_6H_6	45
6	**1**	TMS_2O	23
7	**1**	CPME	44
8	**1**	*n*-pentane	12
9	**1**	1,4-dioxane	19

[a]Determined by ^{1}H NMR integration against internal standard CH_2Br_2.

The dehalogenation of $PhCH_2Cl$ proceeded much slower with **1-^{i}Pr** and **1-Cy** despite their longer lifetimes than **1**. This difference was attributed to steric congestion from the guanidinate ligands which disfavored coordination at the Ce(III) cation.

We also reasoned that the aminyl radical could be harnessed for hydrogen atom abstraction reactions. This objective was achieved using more challenging substrates containing C(sp^2)−X bonds. Irradiation of a 20 mol % solution of **1** with 4-F-C_6H_4X (X = I, Br) and $NaN(SiMe_3)_2$ in benzene at room temperature for 6 d afforded 1-(4-fluorophenyl)benzene in 68% and 43% isolated yields for X = I and Br, respectively (Scheme 4), while no reaction was observed for X = Cl (Figure S27). The identity of the biphenyl product was also confirmed by ^{19}F NMR spectroscopy as well as high resolution mass spectrometry

Scheme 2. Photoinduced Oxidation of 1, 1-^{i}Pr, and 1-Cy with $PhCH_2Cl$

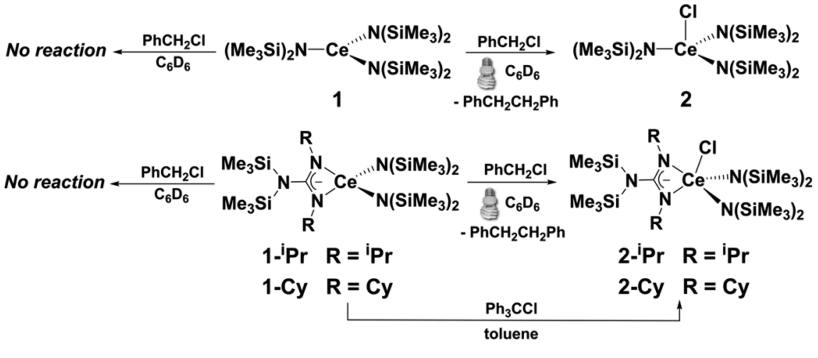

DOI: 10.1021/jacs.5b05411
J. Am. Chem. Soc. 2015, 137, 9234−9237

Scheme 4. Catalytic Arylations of Benzene with ArX (X = I, Br)

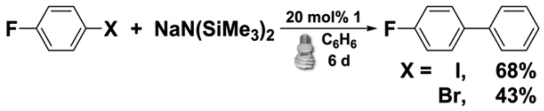

(HRMS). The origin of the phenyl group was confirmed with the use of deuterobenzene as the reaction solvent; the molecular mass corresponding to 1-(4-fluorophenyl)-2,3,4,5,6-deuterobenzene was detected by HRMS (see Figure S29). Direct $C(sp^2)-H$ and $C(sp^2)-X$ couplings in the presence of catalytic 1,10-phenanthroline derivatives at elevated temperatures were reported recently by Shi and Hayashi[17] and were proposed to proceed through a single electron transfer (SET) mechanism. In our case, NMR-scale reactions of **1** with excess 4-F-C_6H_4Br in C_6D_6 revealed the formation of $Ce^{IV}Br[N(SiMe_3)_2]_3$.[18] Therefore, the catalytic generation of the biphenyl products was rationalized through an $S_{RN}1$-type mechanism comprising the following: (1) photoinduced halogen abstraction from 4-F-C_6H_4Br by **1** leading to $Ce^{IV}Br[N(SiMe_3)_2]_3$ and 4-F-C_6H_4·; (2) addition of 4-F-C_6H_4· to benzene forming the radical adduct; (3) salt metathesis and reduction of $Ce^{IV}Br[N(SiMe_3)_2]_3$ with $NaN(SiMe_3)_2$ to regenerate **1** and form $\cdot N(SiMe_3)_2$; (4) hydrogen atom abstraction of the radical adduct by $\cdot N(SiMe_3)_2$ to give the biphenyl product (see Scheme S2 for proposed catalytic cycle). These reactions were catalytic in **1** and demonstrated for the first time that an f-block complex could serve as an effective molecular photoredox catalyst.

Through combined spectroscopic and computational studies, we demonstrated luminescent Ce(III) complexes **1**, **1-^{i}Pr**, and **1-Cy** possess singly occupied $5d_{z^2}$ orbitals in their long-lived excited states. The metalloradical nature of the excited states allowed electrophilic cerium(III) complexes to act as photosensitizers that activated challenging substrates through inner sphere processes, taking advantage of the enthalpy gain in the formation of Ce(IV)−X bonds. A drawback in the current system is the relatively low absorptivity of Ce(III) complexes, which limits the catalytic turnover rates. Development of new sensitized cerium(III) photoredox catalysts, expanded reactivity studies, and physicochemical studies on cerium(III) luminescence characteristics are currently underway in our laboratory.

■ ASSOCIATED CONTENT

Supporting Information

Crystallographic data (CIF), electrochemical data, electronic absorption data, excitation and emission data, computational details, and optimization data for catalysis. The Supporting Information is available free of charge on the ACS Publications website at DOI: 10.1021/jacs.5b05411.

■ AUTHOR INFORMATION

Corresponding Authors

*jmanna@sas.upenn.edu
*schelter@sas.upenn.edu

Notes

The authors declare no competing financial interest.

■ ACKNOWLEDGMENTS

We gratefully acknowledge the University of Pennsylvania and the National Science Foundation (CHE-1362854) for financial support. This work used the Extreme Science and Engineering Discovery Environment (XSEDE), which is supported by U.S. NSF Grant Number OCI-1053575. We thank the E. J. Petersson and S. J. Park groups at UPenn for use of their fluorometers.

■ REFERENCES

(1) Kalyanasundaram, K. *Coord. Chem. Rev.* **1982**, *46*, 159.
(2) Dixon, I. M.; Collin, J.-P.; Sauvage, J.-P.; Flamigni, L.; Encinas, S.; Barigelletti, F. *Chem. Soc. Rev.* **2000**, *29*, 385.
(3) (a) Sattler, W.; Ener, M. E.; Blakemore, J. D.; Rachford, A. A.; LaBeaume, P. J.; Thackeray, J. W.; Cameron, J. F.; Winkler, J. R.; Gray, H. B. *J. Am. Chem. Soc.* **2013**, *135*, 10614. (b) Sattler, W.; Henling, L. M.; Winkler, J. R.; Gray, H. B. *J. Am. Chem. Soc.* **2015**, *137*, 1198.
(4) (a) Kern, J.-M.; Sauvage, J.-P. *J. Chem. Soc., Chem. Commun.* **1987**, 546. (b) Harkins, S. B.; Peters, J. C. *J. Am. Chem. Soc.* **2005**, *127*, 2030.
(5) Ghosh, I.; Ghosh, T.; Bardagi, J. I.; König, B. *Science* **2014**, *346*, 725.
(6) (a) Zeitler, K. *Angew. Chem., Int. Ed.* **2009**, *48*, 9785. (b) Yoon, T. P.; Ischay, M. A.; Du, J. *Nat. Chem.* **2010**, *2*, 527. (c) Narayanam, J. M. R.; Stephenson, C. R. J. *Chem. Soc. Rev.* **2011**, *40*, 102. (d) Prier, C. K.; Rankic, D. A.; MacMillan, D. W. C. *Chem. Rev.* **2013**, *113*, 5322. (e) Xi, Y.; Yi, H.; Lei, A. *Org. Biomol. Chem.* **2013**, *11*, 2387. (f) Tellis, J. C.; Primer, D. N.; Molander, G. A. *Science* **2014**, *345*, 433.
(7) Nguyen, J. D.; D'Amato, E. M.; Narayanam, J. M. R.; Stephenson, C. R. J. *Nat. Chem.* **2012**, *4*, 854.
(8) Piro, N. A.; Robinson, J. R.; Walsh, P. J.; Schelter, E. J. *Coord. Chem. Rev.* **2014**, *260*, 21.
(9) (a) Aspinall, H. C. *Chemistry of the f-Block Elements*; CRC Press: 2001; p 34. (b) Cotton, S. *Lanthanide and Actinide Chemistry*; John Wiley and Sons: West Sussex, U.K., 2006; pp 61−77.
(10) (a) Rausch, M. D.; Moriarty, K. J.; Atwood, J. L.; Weeks, J. A.; Hunter, W. E.; Brittain, H. G. *Organometallics* **1986**, *5*, 1281. (b) Hazin, P. N.; Bruno, J. W.; Brittain, H. G. *Organometallics* **1987**, *6*, 913. (c) Hazin, P. N.; Lakshminarayan, C.; Brinen, L. S.; Knee, J. L.; Bruno, J. W.; Streib, W. E.; Folting, K. *Inorg. Chem.* **1988**, *27*, 1393. (d) Zheng, X.-L.; Liu, Y.; Pan, M.; Lü, X.-Q.; Zhang, J.-Y.; Zhao, C.-Y.; Tong, Y.-X.; Su, C.-Y. *Angew. Chem., Int. Ed.* **2007**, *46*, 7399.
(11) (a) Tretiak, S.; Saxena, A.; Martin, R. L.; Bishop, A. R. *Chem. Phys. Lett.* **2000**, *331*, 561. (b) Martin, R. L. *J. Chem. Phys.* **2003**, *118*, 4775.
(12) (a) Fieser, M. E.; MacDonald, M. R.; Krull, B. T.; Bates, J. E.; Ziller, J. W.; Furche, F.; Evans, W. J. *J. Am. Chem. Soc.* **2015**, *137*, 369. (b) MacDonald, M. R.; Bates, J. E.; Ziller, J. W.; Furche, F.; Evans, W. J. *J. Am. Chem. Soc.* **2013**, *135*, 9857. (c) Langeslay, R. R.; Fieser, M. E.; Ziller, J. W.; Furche, F.; Evans, W. J. *Chem. Sci.* **2015**, *6*, 517. (d) MacDonald, M. R.; Fieser, M. E.; Bates, J. E.; Ziller, J. W.; Furche, F.; Evans, W. J. *J. Am. Chem. Soc.* **2013**, *135*, 13310.
(13) (a) Rehm, D.; Weller, A. *Isr. J. Chem.* **1970**, *8*, 259. (b) Tucker, J. W.; Stephenson, C. R. J. *J. Org. Chem.* **2012**, *77*, 1617.
(14) Williams, U. J.; Robinson, J. R.; Lewis, A. J.; Carroll, P. J.; Walsh, P. J.; Schelter, E. J. *Inorg. Chem.* **2014**, *53*, 27.
(15) Grimshaw, J. *Electrochemical reactions and mechanisms in organic chemistry*; Elsevier Science B. V.: 2000; p 99.
(16) (a) Dröse, P.; Hrib, C. G.; Edelmann, F. T. *J. Organomet. Chem.* **2010**, *695*, 1953. (b) Dröse, P.; Crozier, A. R.; Lashkari, S.; Gottfriedsen, J.; Blaurock, S.; Hrib, C. G.; Maichle-Mössmer, C.; Schädle, C.; Anwander, R.; Edelmann, F. T. *J. Am. Chem. Soc.* **2010**, *132*, 14046. (c) Werner, D.; Deacon, G. B.; Junk, P. C.; Anwander, R. *Chem. - Eur. J.* **2014**, *20*, 4426.
(17) (a) Shirakawa, E.; Itoh, K.-i.; Higashino, T.; Hayashi, T. *J. Am. Chem. Soc.* **2010**, *132*, 15537. (b) Sun, C.-L.; Li, H.; Yu, D.-G.; Yu, M.; Zhou, X.; Lu, X.-Y.; Huang, K.; Zheng, S.-F.; Li, B.-J.; Shi, Z.-J. *Nat. Chem.* **2010**, *2*, 1044. (c) Li, H.; Sun, C.-L.; Yu, M.; Yu, D.-G.; Li, B.-J.; Shi, Z.-J. *Chem. - Eur. J.* **2011**, *17*, 3593. (d) Sun, C.-L.; Gu, Y.-F.; Huang, W.-P.; Shi, Z.-J. *Chem. Commun.* **2011**, *47*, 9813.
(18) Williams, U. J.; Carroll, P. J.; Schelter, E. J. *Inorg. Chem.* **2014**, *53*, 6338.

DOI: 10.1021/jacs.5b05411
J. Am. Chem. Soc. 2015, 137, 9234−9237